

# Reactivation of epigenetically silenced miR-512 and miR-373 sensitizes lung cancer cells to cisplatin and restricts tumor growth

S Adi Harel<sup>1,5</sup>, N Bossel Ben-Moshe<sup>2,5</sup>, Y Aylon<sup>1</sup>, DR Bublik<sup>1</sup>, N Moskovits<sup>1</sup>, G Toperoff<sup>3</sup>, D Azaiza<sup>3</sup>, F Biagoni<sup>4</sup>, G Fuchs<sup>1</sup>, S Wilder<sup>1</sup>, A Hellman<sup>3</sup>, G Blandino<sup>4</sup>, E Domany<sup>2</sup> and M Oren<sup>\*1</sup>

**MicroRNAs (miRs) regulate a variety of cellular processes, and their impaired expression is involved in cancer. Silencing of tumor-suppressive miRs in cancer can occur through epigenetic modifications, including DNA methylation and histone deacetylation. We performed comparative miR profiling on cultured lung cancer cells before and after treatment with 5'aza-deoxycytidine plus Trichostatin A to reverse DNA methylation and histone deacetylation, respectively. Several tens of miRs were strongly induced by such 'epigenetic therapy'. Two representatives, miR-512-5p (miR-512) and miR-373, were selected for further analysis. Both miRs were secreted in exosomes. Re-expression of both miRs augmented cisplatin-induced apoptosis and inhibited cell migration; miR-512 also reduced cell proliferation. *TEAD4* mRNA was confirmed as a direct target of miR-512; likewise, miR-373 was found to target *RelA* and *PIK3CA* mRNA directly. Our results imply that miR-512 and miR-373 exert cell-autonomous and non-autonomous tumor-suppressive effects in lung cancer cells, where their re-expression may benefit epigenetic cancer therapy.**

*Cell Death and Differentiation* (2015) 22, 1328–1340; doi:10.1038/cdd.2014.221; published online 16 January 2015

Lung cancer is the leading cause of cancer-related deaths worldwide (American Cancer Society, Cancer Facts and Figures 2014). In contrast to several other types of cancers, there has been almost no improvement in the 5-year survival rates of lung cancer patients in the past years, and they remain about 16% (American Cancer Society, Cancer Facts and Figures 2014), partially because of acquired resistance to existing therapies.<sup>1</sup> Clinically, lung cancer is divided broadly into small cell lung cancer and non-small cell lung cancer, the latter comprising about 84% of all cases.<sup>2</sup> In recent years, the involvement of epigenetic processes, particularly those resulting in silencing of key regulatory genes, has been firmly established.<sup>3</sup> A major mechanism of epigenetic silencing involves DNA hypermethylation, particularly of CpG islands in the vicinity of gene promoters and enhancers.<sup>4,5</sup> Histone deacetylases (HDACs) recruited to the methylated cytosines can create a closed chromatin state that is less accessible for transcription.<sup>6</sup> Compounds such as 5'aza-2'-deoxycytidine (5'aza) can reverse CpG island hypermethylation by inactivating DNA methyltransferases. 5'aza is often used in combination with HDAC inhibitors such as Trichostatin A (TSA), to induce the re-expression of epigenetically silenced genes.<sup>7</sup>

MicroRNAs (miRs) are small noncoding RNAs that inhibit protein expression by posttranscriptional inhibition. They are fundamental regulators of diverse cellular processes, whose deregulation contributes to many human diseases including

cancer.<sup>8</sup> Notably, miRs can play critical roles in cancer initiation and progression, and deregulated miR expression is frequently observed in human cancers.<sup>9,10</sup>

Changes in DNA methylation status have been implicated in cancer-associated miR deregulation.<sup>11–13</sup> As a single miR often inhibits numerous mRNAs within a defined biological pathway, understanding the epigenetic regulation of miRs in cancer might facilitate the development of new cancer therapies.

In the present study, we set out to identify miRs silenced in lung cancer cells by DNA hypermethylation in a manner that may contribute to resistance to cisplatin. We found that inhibition of epigenetic silencing caused upregulation of two miR clusters located on chromosome 19: the C19MC (ch19 miR cluster) and the miR-371-373 cluster, both associated with human embryonic stem cells.<sup>14</sup> We subsequently focused on one representative miR from each cluster: miR-512-5p (miR-512) and miR-373, respectively. We report that both miRs can exert negative effects on lung cancer cells, including induction of apoptosis and inhibition of cell migration. *RelA* and *PIK3CA* were identified as direct miR-373 targets and *TEAD4* as a miR-512 target, whose downregulation may underpin some of the anti-tumoral effects of those miRs. Thus, epigenetic cancer therapy may operate partly via reactivation of silenced miRs.

<sup>1</sup>Department of Molecular Cell Biology, Weizmann Institute of Science, Rehovot 76100, Israel; <sup>2</sup>Department of Physics of Complex Systems, Weizmann Institute of Science, Rehovot 76100, Israel; <sup>3</sup>Department of Developmental Biology and Cancer Research, Institute for Medical Research Israel-Canada, Hebrew University-Hadassah Medical School, Jerusalem 91120, Israel and <sup>4</sup>Translational Oncogenomic Unit, Regina Elena National Cancer Institute, Rome, Italy

\*Corresponding author: M Oren, Department of Molecular Cell Biology, Weizmann Institute of Science, 234 Herzl Street, Rehovot 7610001 Israel. Tel: +972 8 934 2358; Fax: +972 8 934 6004; E-mail: moshe.oren@weizmann.ac.il

<sup>5</sup>These authors contributed equally to this work.

**Abbreviations:** miRs, microRNAs; HDAC, histone deacetylase; 5'aza, 5'aza-2'-deoxycytidine; TSA, Trichostatin A; C19MC, chromosome 19 miR cluster; HBECs, human bronchial epithelial cells

Received 24.7.14; revised 23.11.14; accepted 24.11.14; Edited by K Vousden; published online 16.1.15

## Results

### Genomewide erasure of DNA methylation in A549 lung cancer cells induces cell death and senescence.

Changes in DNA methylation have been correlated with altered miR expression in cancer.<sup>11,12</sup> To examine the effect of genomewide reversal of DNA hypermethylation and histone deacetylation on miR expression patterns, we treated A549 lung cancer cells for 72 h with a combination of 5'aza and TSA. Cisplatin was then added for an additional 48 h, at which time cells were harvested for FACS-based cell cycle analysis and miR microarray profiling. Cisplatin triggered apoptotic cell death (larger sub-G<sub>1</sub> population), as well as prominent G<sub>2</sub>/M cell cycle arrest (Figure 1a). 5'aza+TSA elicited a milder increase in both sub-G<sub>1</sub> and G<sub>2</sub>/M. Remarkably, combining 5'aza+TSA with cisplatin resulted in a substantial increase in apoptosis, while compromising the G<sub>2</sub>/M arrest. Hence, genomewide erasure of DNA methylation may facilitate the effective activation of cell death pathways in cancer cells exposed to genotoxic chemotherapy, or increase the fraction of responsive cells. Intriguingly, depletion of the p53 tumor suppressor did not affect significantly the outcome of the epigenetic treatment (data not shown).

The ability of cells to migrate is a prerequisite for cancer invasion and metastasis.<sup>15</sup> To assess the impact of epigenetic treatment on cell migration, A549 cells were treated with 5'aza+TSA and monitored for 25 h in a Real Time Cell Analyzer system. As seen in Figure 1b, this treatment had a pronounced

inhibitory effect on cell migration, suggesting a possible mechanism of anticancer activity.

Cellular senescence can act as a tumor inhibitory mechanism.<sup>16,17</sup> To assess whether epigenetic treatment affects cellular senescence, A549 cells were subjected to three 96 h cycles of 5'aza+TSA treatment and stained for senescence-associated beta galactosidase, a commonly used senescence marker. As seen in Figure 1c, treated cells displayed much stronger staining than control cells, along with enlarged flattened morphology. Thus, epigenetic therapy can drive lung cancer cells towards senescence. The ability of senescent cells to induce and maintain cell cycle arrest is largely based on suppression of the E2F transcription factor by active Rb tumor suppressor protein.<sup>17</sup> Indeed, whereas control A549 cells expressed abundant phospho-Rb, indicative of its inactivation, 5'aza+TSA-treated cells displayed only dephosphorylated, presumably active Rb (Supplementary Figure S1A). Furthermore, senescent cells produce inflammatory cytokines, a phenomenon known as Senescence-Associated Secretory Phenotype.<sup>16</sup> Indeed, 5'aza+TSA-treated cells expressed significantly elevated mRNA levels of *IL-6*, a Senescence Associated Secretory Phenotype component (Supplementary Figure S1B).

Although TSA is widely employed for research, it is not in clinical use. The HDAC inhibitor Vorinostat (SAHA) is approved for treatment of cutaneous T-cell lymphoma, and is presently in clinical trials for lung cancer.<sup>18</sup> As seen in Supplementary Figure S2D, the cell cycle effects of 5'aza+SAHA resembled those of 5'aza+TSA.

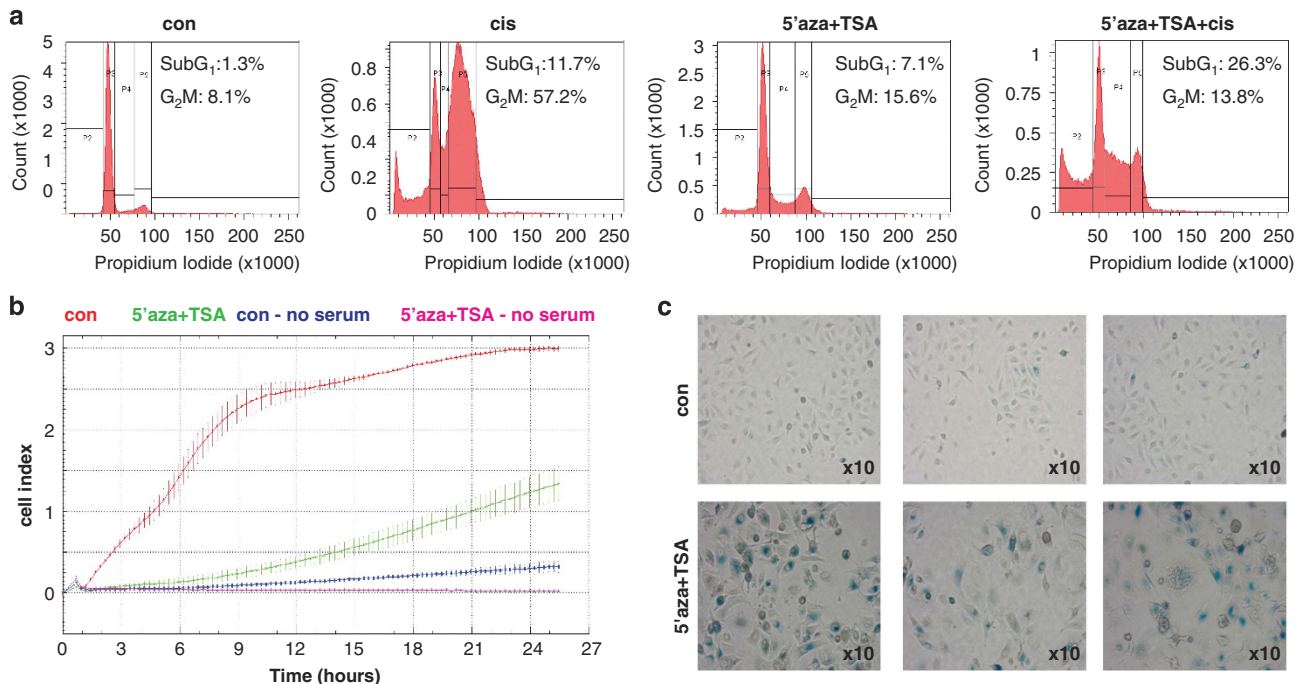


**Figure 1** 5'aza+TSA treatment of A549 cells promotes apoptosis and senescence and inhibits migration. (a) A549 lung cancer cells were treated with a combination of 1  $\mu$ M 5'aza+0.1  $\mu$ M TSA for 72 h. Next, 40 ng/ml cisplatin (cis) was added for an additional 48 h and cells were subjected to cell cycle analysis by flow cytometry,  $n=3$ . (b) A549 cells were subjected to three 96-h cycles of 5'aza+TSA or acetic acid as control. Cycles were separated by 48 h of cultivation in regular medium. At the end of the treatment, cells were seeded in transwells and migration was measured every 15 min in a Real Time Cell Analyzer (see Materials and Methods). Bars represent mean  $\pm$  S.D. of duplicates in the same experiment,  $n=2$ . (c) Representative images of  $\beta$ -gal staining. A549 cells were treated as in (b) and then subjected to  $\beta$ -gal staining

**5'aza+TSA treatment induces expression of two chromosome 19 miR clusters.** A549 cells treated with 5'aza+TSA and/or cisplatin were subjected to miR profiling. Twenty-nine miRs were strongly upregulated (variance > 0.2) by 5'aza+TSA (Figure 2a). Another 32 miRs were downregulated (variance > 0.2), perhaps via an indirect mechanism involving induction of transcriptional repressors (Supplementary Table S1). Notably, 14 of the 29 ( $P = 2.51 \times 10^{-9}$ ) strongly induced miRs belong to two miR clusters, the C19MC cluster and the miR 371-373 cluster, both on chromosome 19. The array included probes for 32 miRs residing within these clusters; 31 of the 32 miRs were upregulated at least to some extent by 5'aza+TSA (Figure 2b).

C19MC is a primate-specific cluster comprising 46 tandemly repeated miRs.<sup>19</sup> It is epigenetically suppressed in human gastric cancer cell lines, and expression of several of its resident miRs was restored by 5'aza treatment.<sup>19</sup> The miR 371-373 cluster, expressed in human embryonic stem cells, is involved in stem cell pluripotency.<sup>20</sup> We subsequently chose to focus on one representative of each cluster: miR-512-5p (miR-512), belonging to the C19MC cluster, and miR-373. qRT-PCR analysis confirmed that miR-512 and miR-373, both nearly undetectable in A549 cells, were highly induced by 5'aza+TSA (Figures 2c and d). Cisplatin partly reduced the levels of both miRs, which nevertheless remained greatly elevated. Conceivably, these miRs cooperate with canonical cisplatin-induced proapoptotic genes such as *Bax* and *CD95* (Supplementary Figure S2A) to augment apoptosis. We propose that combining cisplatin together with 5'aza+TSA provides a setting where both the miRs and the proapoptotic protein-coding genes are upregulated concurrently, maximizing their joint contribution to apoptosis (Figures 2c and d and Supplementary Figure S2A).

5'aza+TSA treatment upregulated strongly the levels of the primary transcripts (pri-miRs) of miR-512-1 and miR-373 (Supplementary Figure S2B and S2C), arguing that induction of those miRs occurs at the transcriptional level. Curiously, pri-miR-512-2 was not induced by 5'aza+TSA (data not shown). Like 5'aza+TSA, 5'aza+SAHA also induced miR-512 and miR-373 (Supplementary Figure S2D). Induction of both miRs was observed also in other lung cancer cell lines (Supplementary Figure S3A). Remarkably, those miRs were not induced to a comparable extent in human bronchial epithelial cells (HBECs) immortalized by hTERT/Cdk4 expression (Figure 2e) or in non-transformed MRC5 fetal lung fibroblasts (Supplementary Figure S3A), raising the interesting possibility that in non-cancerous cells, the reversal of epigenetic marks may not suffice to reestablish efficient

expression of at least some silenced miRs. Induction of both miRs, albeit to a lesser extent, was observed also in HCT116 (colorectal carcinoma), HeLa (cervical cancer) and SK-MEL-5 (melanoma) cells (Supplementary Figure S3B).

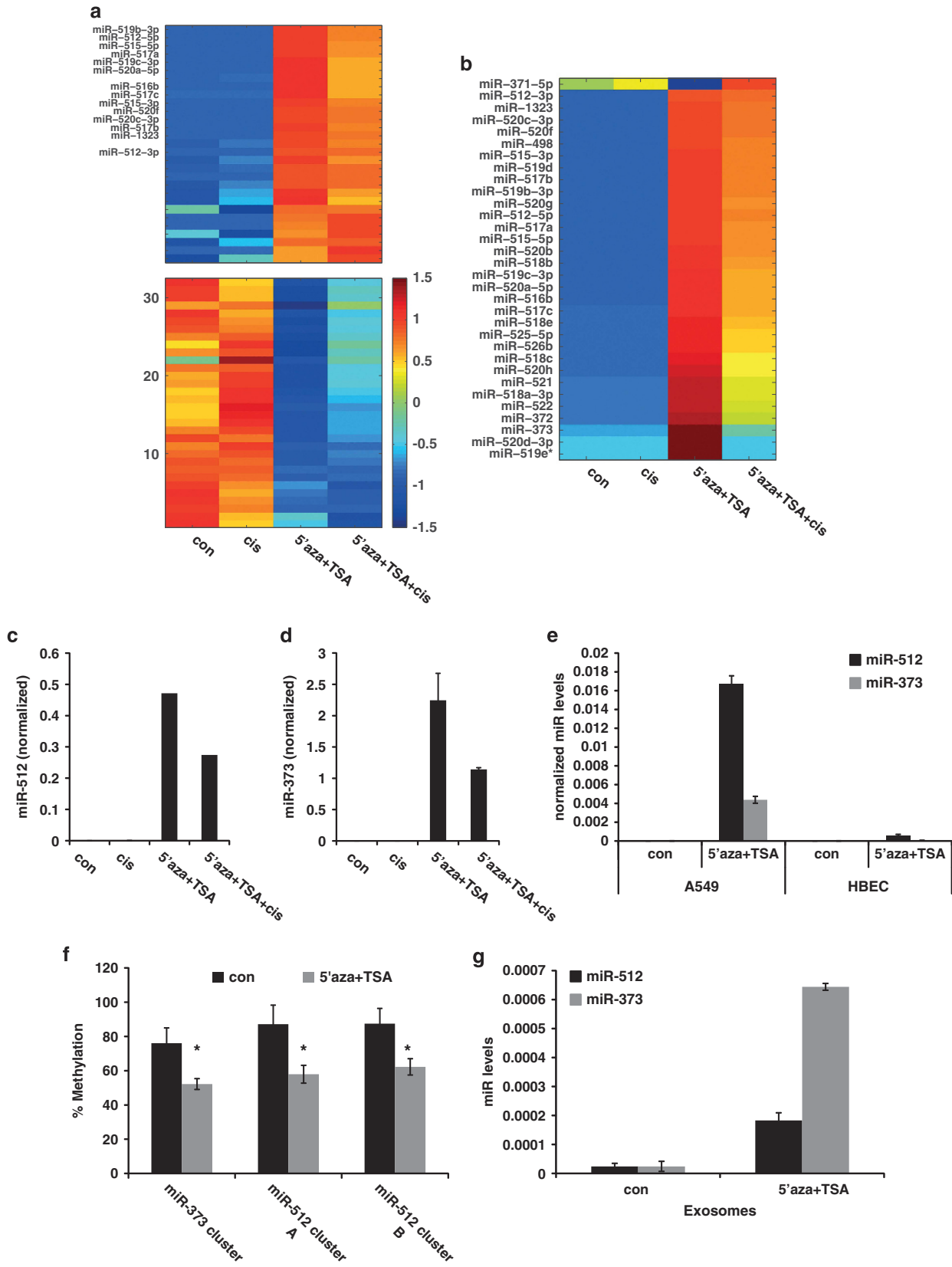
The C19MC cluster is located approximately 17.6 Kb downstream to a CpG-rich region harboring 86 CpG dinucleotide pairs, previously identified as the C19MC promoter region.<sup>19,21</sup> The miR-371-373 cluster is also located downstream to a CpG-rich region identified as part of the miR-373 promoter.<sup>22</sup> To determine whether the putative promoter regions of miR-512 and miR-373 are hypermethylated in A549 cells and whether methylation declines following 5'aza+TSA treatment, genomic DNA from treated and control A549 cells was subjected to bisulfite conversion, followed by amplification of CpG-rich regions of interest and pyrosequencing. As the CpG island of C19MC is long, we employed two different primer sets to amplify it. As seen in Figure 2f, 5'aza+TSA decreased significantly the methylation of all three regions examined. A similar decrease was also observed following combined treatment of 5'aza+TSA together with cisplatin, whereas cisplatin alone had no effect, as expected (Supplementary Figure S3C). Of note, a moderate decline in methylation of a miR promoter suffices to induce its re-expression.<sup>19</sup> Hence, the partial reversal of methylation is probably sufficient to allow re-expression of the miRs populating the two chromosome 19 clusters.

Exosomes are small membrane vesicles of endocytic origin released by cells into their surroundings, which may play a role in cell-cell communication.<sup>23,24</sup> Notably, miRs are part of the exosome cargo, and exosome release is elevated in cancer cells.<sup>24</sup> As shown in Figure 2g, 5'aza+TSA caused a considerable increase in exosomal miR-512 and miR-373.

Together, these results imply that miR-512, miR-373 and their associated miR clusters are silenced by promoter hypermethylation in cancer cells, their expression and secretion being considerably induced upon reversal of epigenetic silencing.

**5'aza+TSA treatment attenuates tumor growth.** To assess the impact of epigenetic treatment on tumor growth, we employed H460 lung cancer cells stably expressing firefly luciferase. In these cells, too, 5'aza+TSA induced both miR-512 and miR-373, albeit to different extents (Figure 3a). Treated and control cells were next injected subcutaneously into nude mice, and tumor growth was monitored by bioluminescence imaging. As seen in Figures 3b and c, prior 5'aza+TSA treatment significantly decreased tumor growth. Remarkably, tumors harvested 16 days post

**Figure 2** miR microarray analysis and validation. (a) Sorting points into neighborhood (Spin)-ordered expression matrix of the most variable miRs across samples, either up- (29) or downregulated (32) in response to 5'aza+TSA treatment; treatment as in (Figure 1a). The 14 miRs identified by name belong to the ch19 cluster and appear also in Figure 2b. Colors indicate expression levels after centering and normalizing each miR (row), with red denoting relatively high expression and blue relatively low expression (see color bar). (b) Spin-ordered expression matrix of 32 miRs of the ch19 clusters measured by the array, across the different samples. Color bar as in (a). (c) qRT-PCR analysis of miR-512, normalized to RNU24. Bars represent mean  $\pm$  S.D. from duplicate qPCR reactions; similar results were obtained in three independent experiments. (d) qRT-PCR analysis of miR-373, normalized to RNU24. Bars represent mean  $\pm$  S.D. from duplicate qPCR reactions; similar results were obtained in three independent experiments. (e) A549 and HBECs were treated with 5'aza+TSA for 72 h and subjected to qRT-PCR analysis. Levels of miR-512 and miR-373 were normalized to RNU24. Bars represent mean  $\pm$  S.D. from duplicate qPCR reactions. (f) Percentage of methylated CpGs as calculated by bisulfite pyrosequencing. Bars represent mean  $\pm$  S.D. from three independent experiments. \* $P$ -value < 0.05. (g) A549 cells were treated with 5'aza+TSA as before. At the end of the treatment, medium was replaced to serum-free medium for 24 h, at which time it was collected and subjected to exosome RNA isolation and qRT-PCR analysis for miR-512 and miR-373. Bars represent mean  $\pm$  S.D. from duplicate qPCR reactions; similar results were obtained in two independent experiments





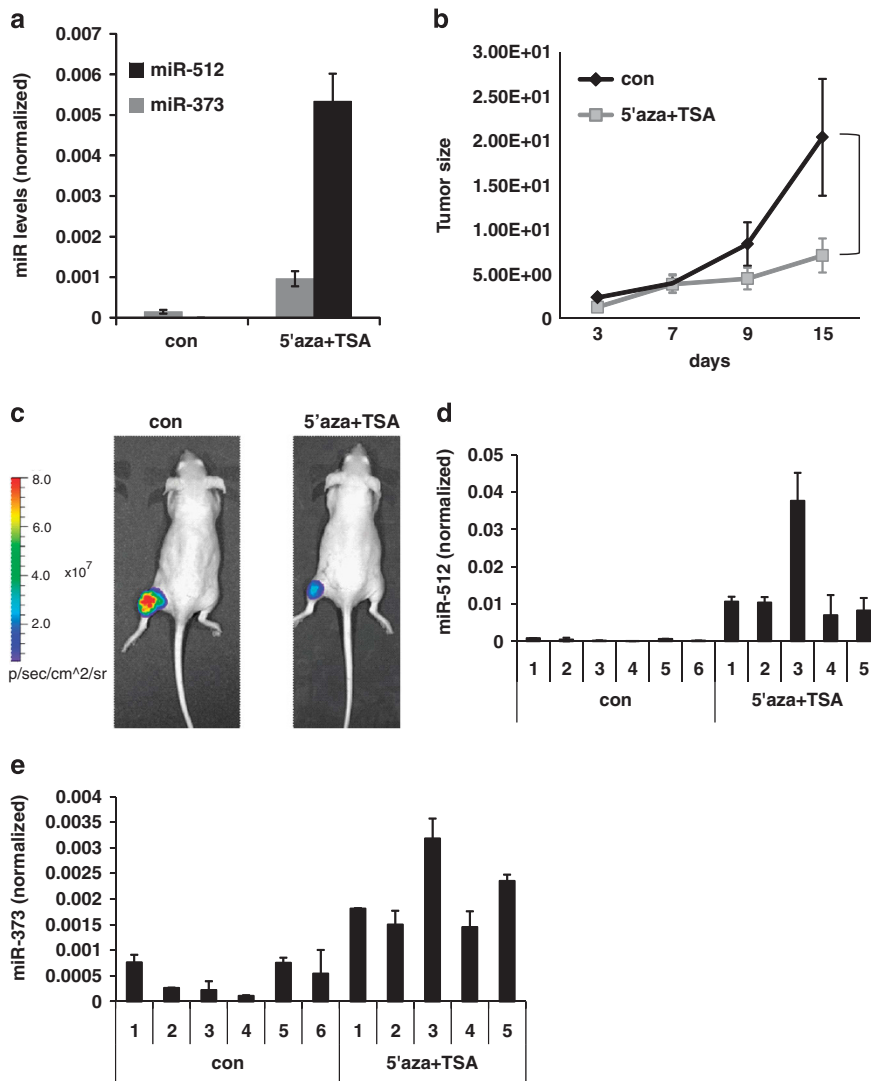


**Figure 3** 5'aza+TSA treatment attenuates tumor growth and induces sustained expression of miR-512 and miR-373. (a) H460 cells stably expressing luciferase were treated with 5'aza+TSA or acetic acid:H<sub>2</sub>O (solvent control) for 72 h and subjected to qRT-PCR analysis. miR-373 and miR-512 were normalized to RNU24. Bars represent mean  $\pm$  S.D. from duplicate qPCR reactions. (b) Cells as in (a) were injected subcutaneously into nude mice. For each time point, the fold change in luciferase bioluminescence intensity of each mouse was calculated relative to the 24 h luciferase signal of the same mouse. The average tumor load of all mice in the same group ( $n = 6$  for control,  $n = 5$  for 5'aza+TSA) was calculated for each time point and plotted. \* $P$ -value  $< 0.05$  at day 15. (c) Representative color-coded luciferase bioluminescence images acquired 15 days after inoculation. (d) qRT-PCR analysis of miR-512 in tumors excised at day 16. Levels are normalized to RNU24. Bars represent mean  $\pm$  S.D. from duplicate qPCR reactions. (e) qRT-PCR analysis of miR-373 in tumors excised at day 16. Levels are normalized to RNU24. Bars represent mean  $\pm$  S.D. from duplicate qPCR reactions

injection retained elevated levels of both miR-512 and miR-373 (Figures 3d and e). Thus, prior 5'aza+TSA treatment efficiently attenuates tumor growth, probably by eliciting long-term modifications in gene expression.

**Re-expression of miR-373 or miR-512 induces cancer cell death and inhibits migration.** To determine whether the re-expression of miR-373 or miR-512 can recapitulate the effects of epigenetic treatment, A549 cells were transfected with the corresponding miR-mimics. Following cisplatin treatment of some cultures for 48 h, cell cycle analysis was performed (Figure 4a). Although overexpression of each miR alone did not cause a detectable change in cell death, both miRs elicited a moderate increase in cisplatin-induced cell

death. Thus, the re-expression of these miRs augments cisplatin cytotoxicity.

Next, colony-formation analysis was performed. Notably, miR-512 overexpression considerably inhibited colony formation, whereas miR-373 had no detectable effect (Figure 4b). Furthermore, BrdU incorporation analysis revealed that miR-512 significantly reduced replicative DNA synthesis, whereas miR-373 had an insignificant stimulatory effect (Figure 4c). Lastly, both miR-512 and miR-373 significantly reduced A549 cell migration (Figure 4d). Thus, reactivation of miR-512 and miR-373 can exert a variety of inhibitory effects in lung cancer cells.

**Identification of miR-512 and miR-373 target genes.** To identify relevant target mRNAs, we subjected control and 5'

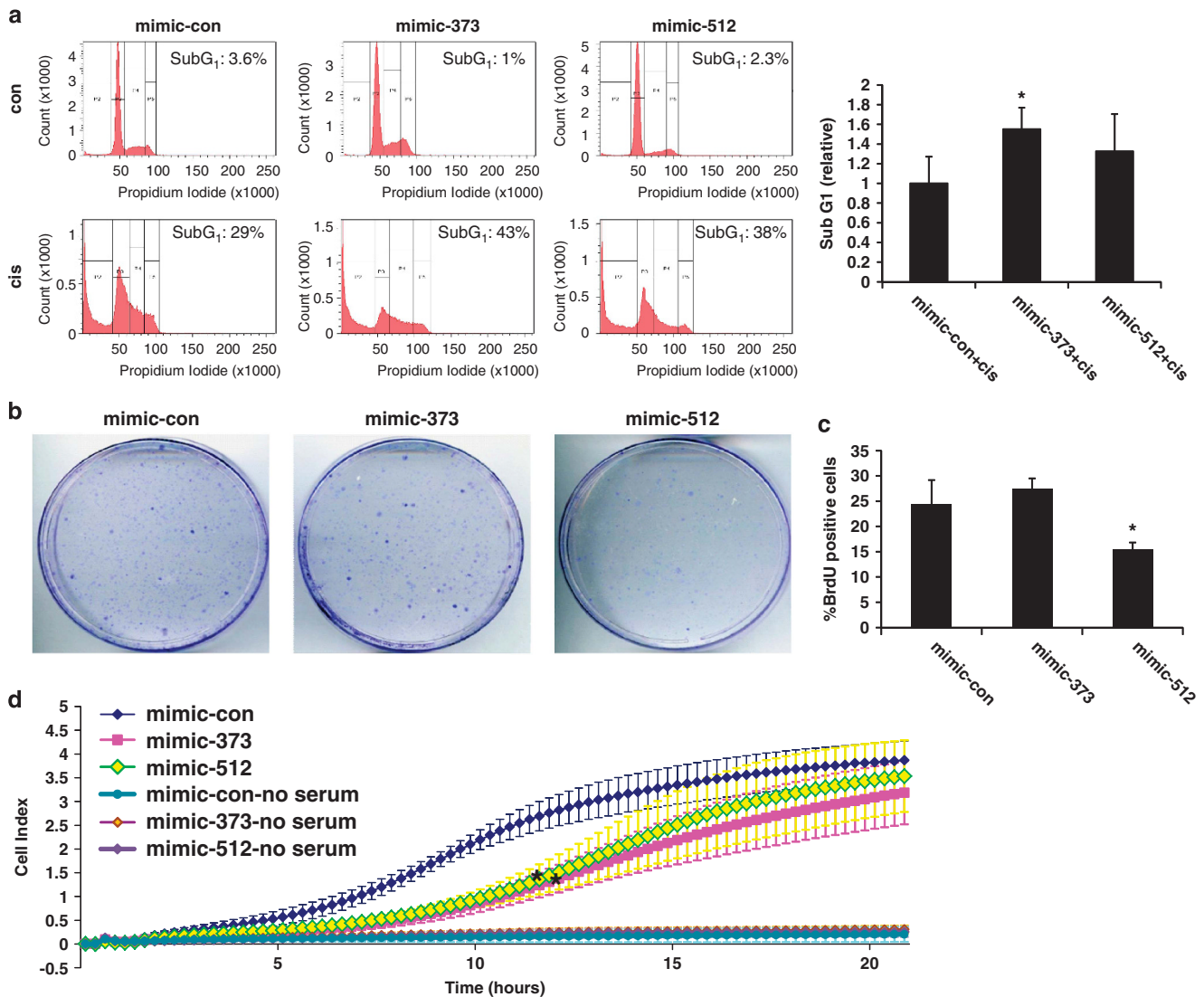


**Figure 4** Biological outcomes of miR-373 and miR-512 overexpression in A549 cells. **(a)** Left: Flow cytometry cell cycle analysis of A549 cells transfected with miR-con, miR-373 mimic or miR-512 mimic oligos and treated with cisplatin for 48 h. Right: Relative sub-G1 fraction following the indicated treatments. The control sample was set as 1. Bars represent mean  $\pm$  S.D. of three independent experiments, \* $P$ -value  $< 0.05$ . **(b)** A colony-formation assay was performed with A549 cells transfected with miR-con, miR-373 mimic or miR-512 mimic oligos. Three weeks after plating, colonies were fixed with methanol and stained with crystal violet,  $n = 3$ . **(c)** Cells were transfected as in **(b)**, and subjected 48 h later to flow cytometry BrdU incorporation analysis; bars represent mean  $\pm$  S.D. of three independent experiments, \* $P$ -value  $< 0.05$ . **(d)** A549 cells transfected with miR-con, miR-373 mimic or miR-512 mimic oligos were seeded in transwells. Migration was monitored every 15 min in a Real Time Cell Analyzer. Bars represent mean  $\pm$  S.D. of three independent experiments, \* $P$ -value  $< 0.05$  (for miR-373 between 1.9 and 20.4 h, for miR-512 between 1.6 and 15.6 h)

aza+TSA-treated samples to gene expression array analysis. As anticipated, many mRNAs were upregulated following epigenetic treatment (Supplementary Figure S4A). Additionally, many other genes were downregulated; this might be due, at least in part, to inhibition of some mRNAs by the re-expressed miRs, including miR-373 or miR-512. One downregulated gene was *Integrin  $\alpha 11$*  (*ITGa11*), overexpressed in more than 80% of non-small cell lung cancer cases.<sup>25</sup> Integrins mediate cell-matrix interactions, stimulate signal transduction, and contribute to cancer cell proliferation, motility and survival.<sup>25</sup> Remarkably, miR-373 overexpression significantly reduced *ITGa11* mRNA (Supplementary Figure S4B). Hence, *ITGa11* mRNA may be a direct miR-373 target.

Unexpectedly, miR-512 overexpression actually increased *ITGa11* levels (data not shown).

To identify more definitively relevant miR-512 and miR-373 targets, A549 cells transfected with miR-512, miR-373 or control oligos were subjected to expression profiling. A total of 1437 and 1197 genes were downregulated at least 1.2-fold following overexpression of miR-512 and miR-373, respectively (Figure 5a). Reassuringly, many of these are predicted (PITA, TargetScan, miRanda) targets of the pertinent miR (Figure 5b). Several known miR-373 targets such as *Lats2*, *CD44* and *TGF $\beta$ R2*<sup>26–28</sup> were also downregulated to different extents in our profiling, strengthening its validity. A total of 488 of the genes downregulated by miR-373 are predicted targets of that miR

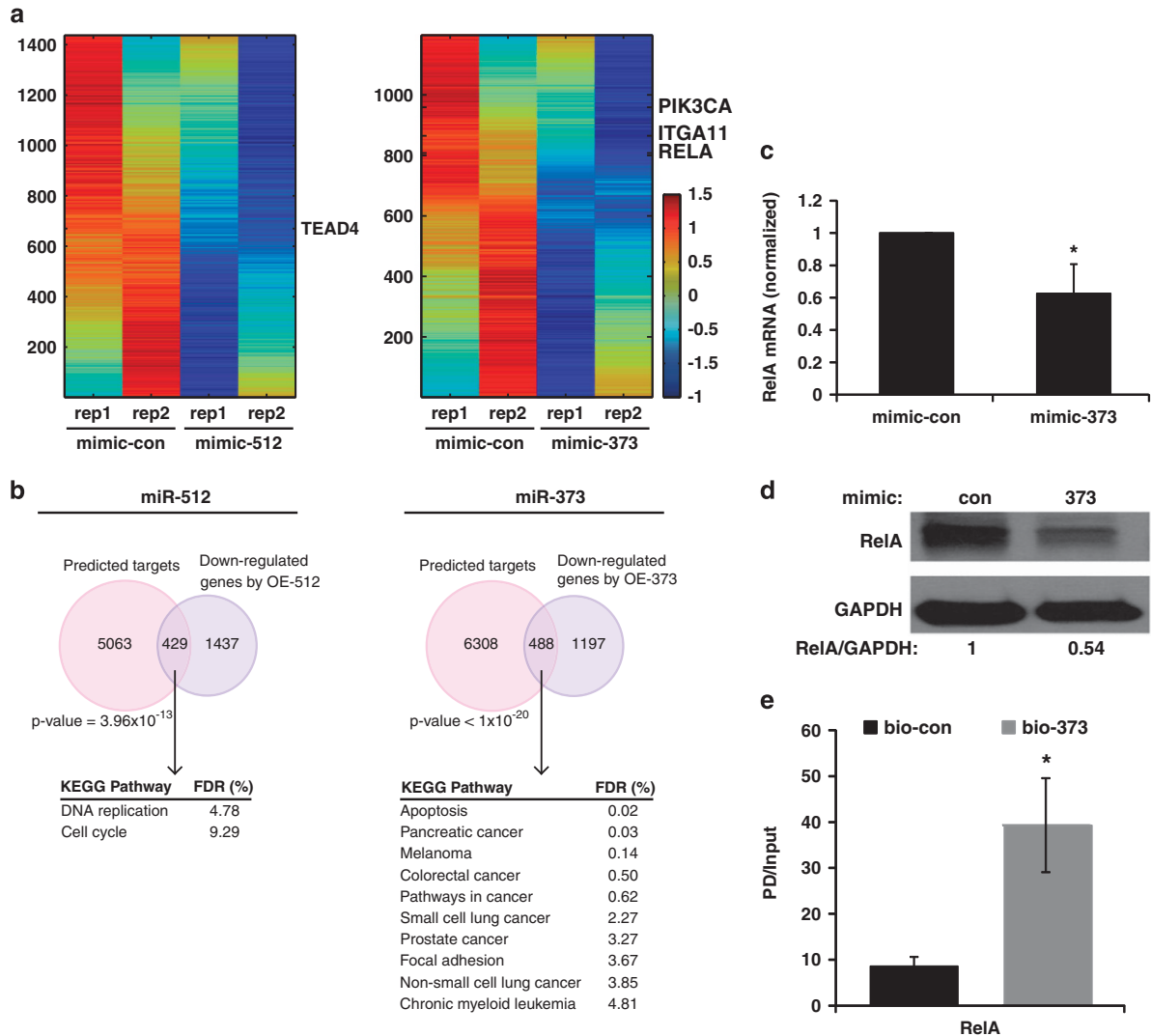


**Figure 5** Identification of miR-512 and miR-373 targets. (a) A549 cells were transfected with miR-con, miR-373 or miR-512 mimic oligos in duplicates and subjected to RNA purification and Affymetrix gene expression profiling. Spin-ordered expression matrix for genes downregulated at least 1.2-fold by overexpression of miR-373 mimic (right) or miR-512 mimic (left) oligos, relative to control miR-mimic,  $n = 2$ . Colors indicate expression levels after centering and normalizing each miR (row), with red denoting relatively high expression and blue relatively low expression (see color bar). (b) Analysis of expression data in (a). Upper panel: Venn diagrams showing the number of target genes predicted by PITA, TargetScan or miRanda sequence-based algorithms, downregulated at least 1.2-fold in both repeats in response to transfection with miR-512 mimic (right) or miR-373 mimic (left). Lower panel: pathways enriched among the downregulated predicted target genes of miR-512 and miR-373. (c) qRT-PCR analysis of *RelA* mRNA in A549 cells transfected with miR-con or miR-373 mimic oligos. Values were first normalized to *GAPDH* mRNA in the same sample and then calculated relative to the mimic-con value, set as 1. Bars represent mean  $\pm$  S.D. from four independent experiments, \* $P$ -value < 0.05. (d) Cells treated as in (c) were subjected to western blot analysis of *RelA* and *GAPDH* proteins,  $n = 3$ . (e) A549 cells were transfected with 100 nM biotinylated miR-373 (bio-373) or biotinylated miR-con (bio-con) and harvested 48 h later for pull-down analysis (see Materials and Methods). Pulled-down (PD) mRNA levels were normalized to *GAPDH* mRNA in the same sample and to input mRNA. Bars represent mean  $\pm$  S.E. of four independent experiments, \* $P$ -value < 0.05

( $P$ -value <  $1 \times 10^{-20}$ ); these genes were enriched for apoptosis, pathways in cancer and focal adhesion (FDR < 10%, Figure 4b right panel).<sup>29,30</sup> Likewise, 429 of the genes downregulated by miR-512 are predicted targets of that miR ( $P$ -value =  $3.96 \times 10^{-13}$ ), and these were enriched for DNA replication and cell cycle (FDR < 10%, Figure 4b left panel), in agreement with the reduced proliferation of miR-512-overexpressing cells (see Figures 4b and c).

One of the genes downregulated by miR-373 and predicted to be targeted by it was *RelA* (*p65*), member of the NF- $\kappa$ B family. The NF- $\kappa$ B transcription factor is involved in diverse processes such as inflammation, cell survival, migration and

invasion.<sup>31</sup> Many tumors, including lung cancers, upregulate NF- $\kappa$ B activity.<sup>31,32</sup> Indeed, miR-373 overexpression caused a significant decrease in *RelA* mRNA (Figure 5c) and protein (Figure 5d), confirming an earlier report.<sup>27</sup> To probe whether the interaction between miR-373 and *RelA* mRNA is direct, as predicted (Supplementary Figure S6A), biotinylated miR-373 was transfected into cells, which were then lysed and the miR-mRNA complexes were captured on streptavidin beads, followed by analysis of the bound mRNA.<sup>33</sup> As shown in Figure 5e, *RelA* mRNA was significantly enriched in the biotin-miR-373 pull-down, implicating *RelA* as a direct miR-373 target.

As miR-373 overexpression augmented cisplatin-induced apoptosis, we wished to assess whether this might be partially explained by RelA inhibition. Indeed, siRNA-mediated RelA downregulation elicited a significant increase in cisplatin-induced apoptosis (Supplementary Figure S5), suggesting that at least some of the apoptotic effect of excessive miR-373 may be due to RelA inhibition.

**miR-373 targets *PIK3CA*.** One transcript downregulated by miR-373 overexpression was *PIK3CA*, encoding the catalytic subunit of PI3 kinase class I, also validated by qRT-PCR (Figure 6a). Furthermore, miR-373 overexpression caused a reduction in PIK3CA protein (Figure 6b). Notably, *PIK3CA* is a predicted miR-373 target (Supplementary Figure S6B).

PI3K family members catalyze phosphorylation of phosphatidylinositol lipids at the 3' position of the inositol ring, producing second messengers that regulate cell growth, survival and motility.<sup>34</sup> The repressive effect of miR-373 was exerted also on a luciferase reporter plasmid harboring the *PIK3CA*-3'UTR (Figure 6c), and *PIK3CA* mRNA was significantly enriched by biotin-miR-373 pulldown (Figure 6d). Both these findings strongly suggest that miR-373 targets directly the *PIK3CA* transcript.

PI3K activity results indirectly in augmented phosphorylation of the Akt/PKB kinase, promoting enhanced proliferation, survival, metabolism, protein synthesis and more.<sup>35</sup> In agreement, miR-373 overexpression reduced Akt phosphorylation without affecting the overall amount of Akt (Figure 6e).

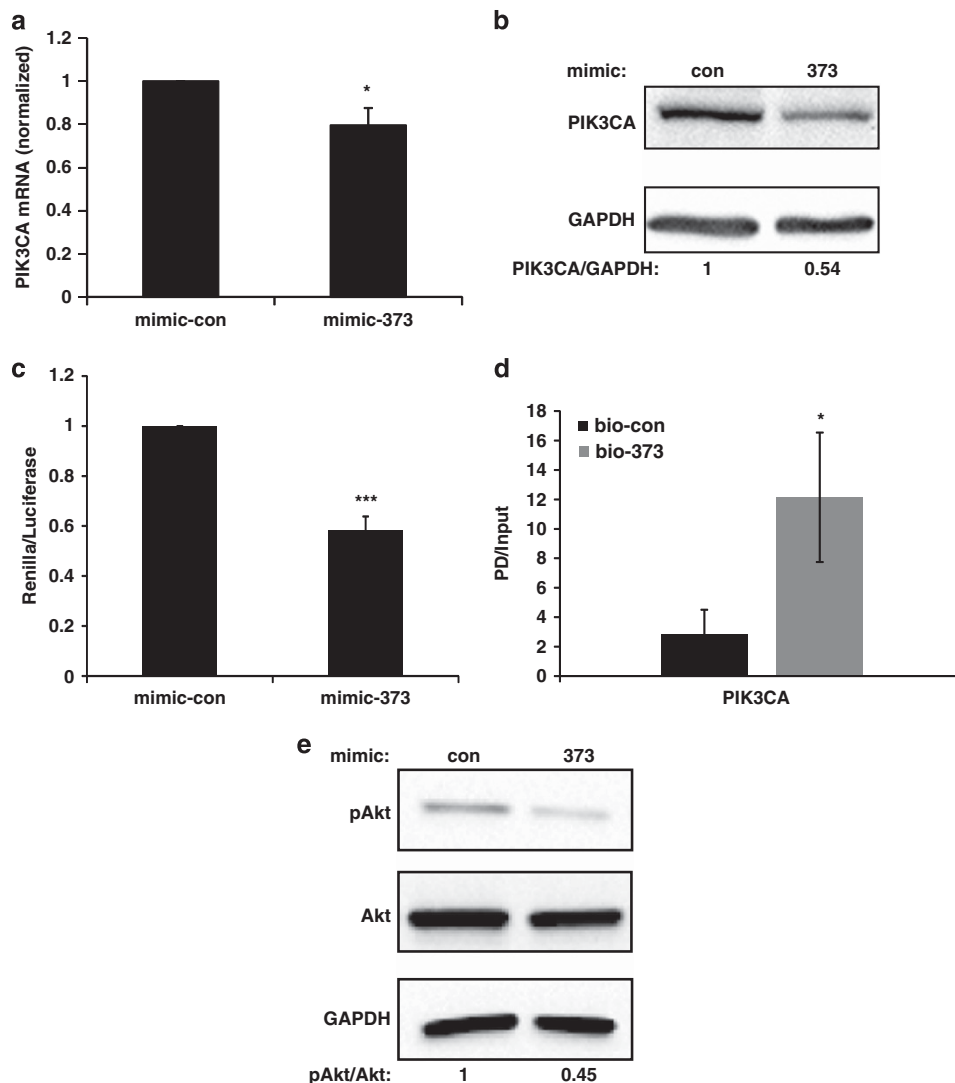


**Figure 6** *PIK3CA* is a direct functional target of miR-373. (a) qRT-PCR analysis of *PIK3CA* mRNA in A549 cells transfected with miR-con or miR-373 mimic oligos. Analysis as in Figure 5c. Bars represent mean  $\pm$  S.D. from three independent experiments, \**P*-value < 0.05. (b) Cells were treated as in (a) and subjected to western blot analysis of *PIK3CA* and *GAPDH* proteins, *n* = 3. (c) A549 cells were transfected with miR-con or miR-373 mimic oligos, and 24 h later transfected again with psiCHECK2 plasmid containing the 3' UTR of *PIK3CA* downstream to the Renilla luciferase reporter gene. After an additional 24 h, cells were lysed and Renilla luciferase activity was measured and normalized to firefly luciferase activity. Bars represent mean  $\pm$  S.E. of three independent experiments, \*\*\**P*-value < 0.0005. (d) miR-373 pulldown. Experimental procedure as in Figure 5e. Bars represent mean  $\pm$  S.E. of five independent experiments, \**P*-value < 0.05. (e) A549 cells were transfected with miR-con or miR-373 mimic oligos and subjected to serum starvation for 20 h, followed by treatment with 10 ng/ml insulin for 10 min. Cells were harvested and subjected to western blot analysis of total *Akt1*, phosphorylated *Akt* (*pAkt*) and *GAPDH*, *n* = 2



Activation of the PI3K/Akt pathway confers chemotherapy resistance.<sup>35</sup> Therefore, inhibition of *PIK3CA* may contribute to the enhanced death of A549 cells upon combined treatment with miR-373 and cisplatin.

**miR-512 targets *TEAD4*.** One of the genes downregulated by miR-512 overexpression was *TEAD4* (Figure 5a), a predicted miR-512 target (Supplementary Figure S6C). Downregulation was validated at both RNA and protein levels (Figures 7a and b). Moreover, luciferase reporter analysis confirmed that the inhibition by miR-512 is mediated via the 3' UTR of *TEAD4* mRNA (Figure 7c). Likewise, biotin-miR-512 pulldown yielded a considerable enrichment of *TEAD4* mRNA (Figure 7d), indicative of direct targeting by miR-512. *TEAD4*, along with other TEAD family members, mediates the activity of the transcriptional co-activator YAP, a positive

regulator of cell proliferation and cell growth and a putative protooncogene.<sup>36</sup> To determine whether miR-512 affects *TEAD4* transcriptional activity, we utilized a luciferase reporter plasmid containing eight tandem TEAD consensus binding site repeats. Indeed, miR-512 overexpression repressed TEAD-dependent transcriptional activity (Figure 7e). As the YAP-TEAD interaction promotes cell proliferation,<sup>37</sup> downregulation of *TEAD4* may contribute to the antiproliferative effect of miR-512 (see Figures 4b and c).

CTGF is a secreted protein whose expression is induced by YAP-TEAD4 transcriptional activity to promote proliferation.<sup>37</sup> Indeed, *CTGF* mRNA was significantly downregulated upon miR-512 overexpression (Figure 7f).

In sum, our findings imply that re-expression of miR-512, miR-373 and their cluster-mates can attenuate tumor-promoting processes in lung cancer cells, partly via targeted

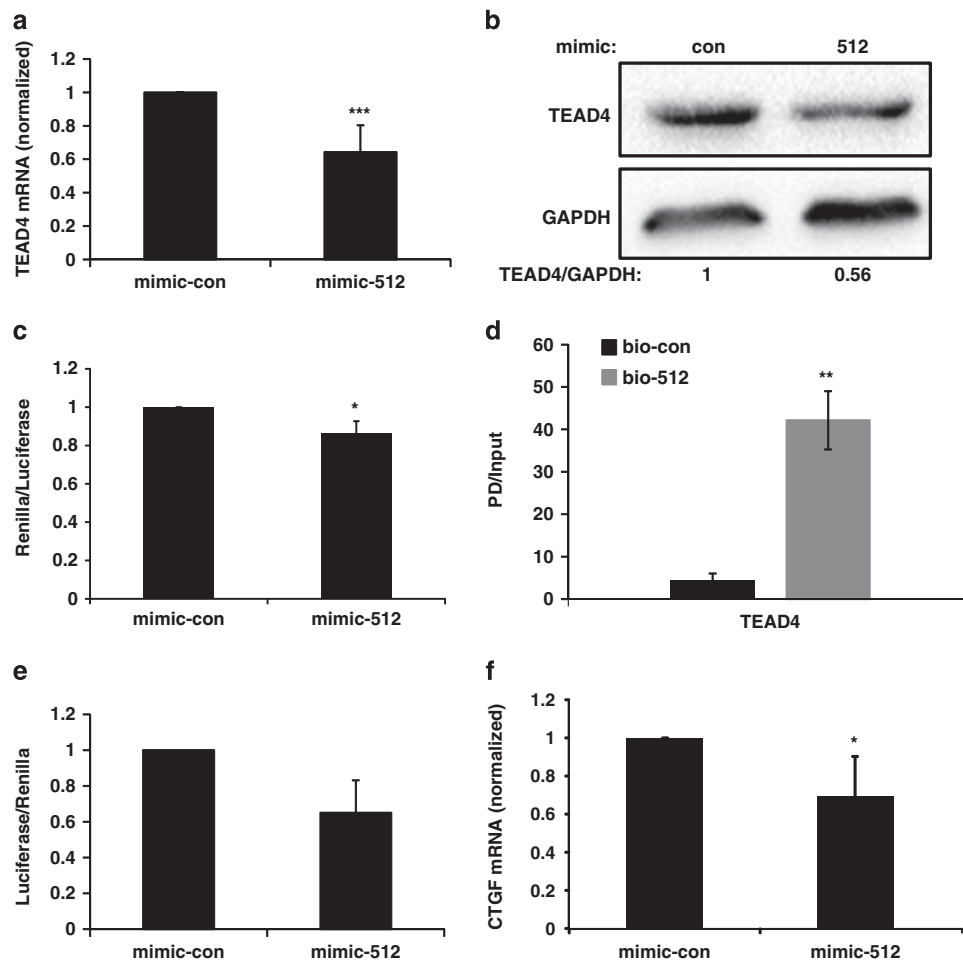


**Figure 7** *TEAD4* is a direct functional target of miR-512. (a) qRT-PCR analysis for *TEAD4* mRNA levels in A549 cells transfected with miR-con or miR-512 mimic oligos. Analysis as in Figure 5c. Bars represent mean  $\pm$  S.D. from six independent experiments, \*\*\**P*-value < 0.0005. (b) Cells transfected as in (a) were subjected to western blot analysis of *TEAD4* and *GAPDH* proteins. (c) A549 cells were transfected with miR-con or miR-512 mimic oligos, and 24 h later transfected again with psiCHECK2 plasmid containing the 3' UTR of *TEAD4* downstream to the Renilla luciferase reporter gene. After an additional 24 h, cells were lysed and Renilla luciferase activity was measured and normalized to firefly luciferase activity. Bars represent mean  $\pm$  S.E. of three independent experiments, \**P*-value < 0.05. (d) A549 cells were transfected with 100 nM biotinylated miR-512 (bio-512) or biotinylated miR-con (bio-con) and harvested 48 h later for pulldown analysis. Analysis as in Figure 5e. Bars represent mean  $\pm$  S.E. of four independent experiments, \*\**P*-value < 0.005. (e) A549 cells were transfected with miR-con or miR-512 mimic oligos, and 24 h later transfected again with PGL3 8xGTIIC and Renilla reporter plasmids. After an additional 24 h, cells were lysed and firefly luciferase activity was measured and normalized to Renilla luciferase activity. Bars represent mean  $\pm$  S.E. of five independent experiments. (f) qRT-PCR analysis of *CTGF* mRNA in A549 cells transfected with control or miR-512 mimic oligos. Analysis as in Figure 5c. Bars represent mean  $\pm$  S.E. from six independent experiments. \**P*-value < 0.05

inhibition of *ITGα11*, *RelA*, *PIK3CA* and *TEAD4* (Figure 8). This inhibition might underpin some of the observed biological effects of the epigenetic treatment.

### Discussion

The fact that the promoter regions of numerous tumor-suppressive genes are methylated in lung cancer, along with the high expression of DNA methyltransferase proteins often observed in such tumors,<sup>38</sup> provide a rationale for using DNA methylation inhibitors, alone or in combination with HDAC inhibitors, for lung cancer treatment. However, past studies with such agents were associated with extensive toxicity and minimal efficacy.<sup>39,40</sup> Hence, it is crucial to obtain better insight into their mode of action in order to increase efficacy and reduce non-specific toxicity.

Here, we demonstrate that the inhibition of DNA methylation and histone deacetylation sensitizes lung cancer cells to cisplatin-induced cell death, extending earlier reports of cytotoxic synergy between epigenetic unsilencing and cisplatin in cancer cells.<sup>41,42</sup> Furthermore, this ‘epigenetic therapy’ induces cancer cell senescence and attenuates cell migration. In agreement with these tissue culture effects, epigenetically treated cells display reduced tumorigenic potential *in vivo*, likely underpinned by epigenetic memory and retention of the alterations elicited by the treatment long after its actual cessation. We further provide evidence that the epigenetic treatment reactivates numerous miRNAs, mostly residing in

chromosome 19, whose expression is effectively silenced in the untreated cancer cells. Notably, overexpression of miR-512 and miR-373, representative members of this large group, partly recapitulates the biological effects of the epigenetic treatment, suggesting that induction of those miRNAs may contribute to the observed inhibitory effects. In line with our results, profiling of miR expression in 357 stage I non-small cell lung cancer patients identified miR-512 as an indicator of good prognosis.<sup>43</sup> High miR-512 expression was associated with better prognosis regardless of cancer subtype. In addition, miR-512 was predictive of better relapse-free survival of lung adenocarcinoma patients. We also identify several new direct targets of miR-512 and miR-373, whose downregulation upon unsilencing of those miRNAs may play a role in the various phenotypic manifestations of the epigenetic treatment. Conceivably, a similar impact on miR reactivation and target mRNA inhibition may facilitate the anti-tumoral effects of combined DNA methyltransferase plus HDAC inhibition in cancer patients.

A recent study, published while this manuscript was under review, also described the epigenetic silencing of miR-373 in A549 cells.<sup>44</sup> However, although we observe that 5’aza alone but not TSA alone suffices to induce miR-373 (data not shown), consistent with a pivotal role of DNA methylation in silencing the corresponding miR cluster, Seol *et al.*<sup>44</sup> reported the opposite that induction of miR-373 occurs only upon TSA treatment but not 5’aza treatment. The reason for this apparent discrepancy is presently unclear.

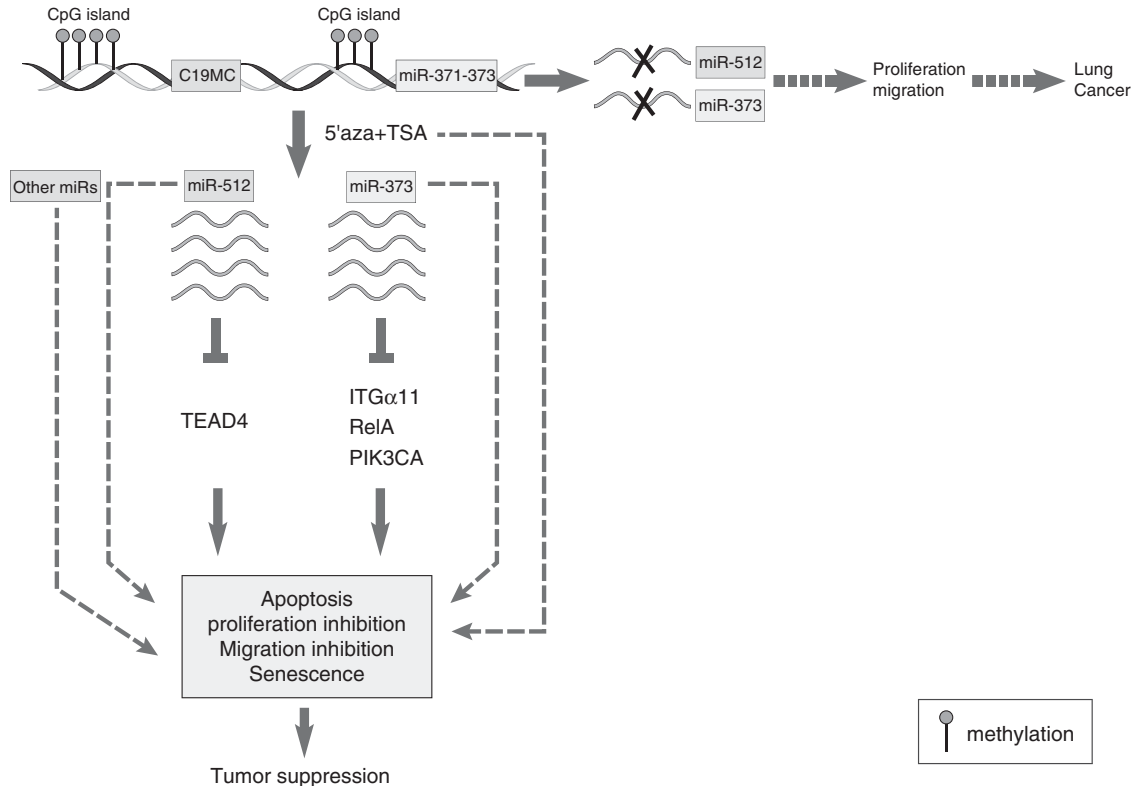


**Figure 8** Schematic representation of the regulatory process proposed in the study. In lung cancer cells, the CpG islands in the vicinity of C19MC (including miR-512) and the miR-371-373 cluster (including miR-373) are highly methylated leading to reduced expression of those miRNAs and contributing to enhanced proliferation and migration. Treatment with 5’aza+TSA reduces CpG island methylation, causing re-expression of the silenced miRNAs. This leads to induction of apoptosis and inhibition of proliferation and cell migration, and may thereby suppress tumor malignancy. These biological outcomes are partially mediated by inhibition of *ITGα11*, *RelA* and *PIK3CA* by miR-373, and of *TEAD4* by miR-512

Interestingly, induction of miR-512 and miR-373 by 5'aza+TSA was observed to varying extents in many human cancer cell lines but less so in non-transformed MRC5 and HBECs. It is tempting to speculate that the lock on expression of the chromosome 19 miR clusters is tighter in normal cells, involving more than just DNA methylation and histone deacetylation, and thus additional mechanisms may be involved in silencing these clusters in such cells. Notably, Liang *et al.*<sup>45</sup> found that almost twice as many genes were induced by 5'aza in human cancer cells as compared with fibroblasts. Likewise, sodium butyrate (HDAC inhibitor) was found to affect the expression of androgen receptor co-regulators only in prostate cancer cells but not in normal prostate cells.<sup>46</sup> These observations are encouraging as they imply that epigenetic therapy might induce genomewide erasure of gene silencing preferentially in tumor cells, reducing the likelihood that such treatment would lead to massive inappropriate gene activation in normal tissues. Yet, it should be kept in mind that the impact of the epigenetic treatment can differ between tumors, and although it could benefit some patients, it might also cause adverse tumor-supportive effects in others.<sup>47</sup> Thus, better criteria for stratifying candidates for epigenetic therapy are strongly needed.

The C19MC and miR-371-373 clusters are located 25 Kb apart on chromosome 19. The picture regarding the biological roles of those miRs and particularly their association with cancer is rather complex. Although the C19MC is silenced by promoter methylation in many cell lines,<sup>19</sup> it is activated together with the miR-371-373 cluster in a subgroup of thyroid adenomas, owing to chromosomal rearrangements.<sup>48</sup> miR-373 was identified by Agami and coworkers<sup>28</sup> as a potential oncogene in testicular germ-cell tumors, partly by targeting the Lats2 tumor suppressor. Later, the same group showed that it promotes breast cancer cell invasion and metastasis by targeting CD44.<sup>26</sup> Furthermore, miR-373 and miR-372 can engage in an oncogenic feedback loop with members of the Wnt/ $\beta$ -catenin pathway.<sup>20</sup> However, although these reports imply that miR-371-373 possess oncogenic activities, other studies reveal that they can display tumor-suppressive features,<sup>22,27,44,49</sup> as observed also here. This dichotomous behavior of miR-373 and other chromosome 19 miRs is not unusual. In fact, there is a growing number of examples where the same miR may have opposing roles in tumorigenesis, depending on the cellular context: the impact of such miRs on cancer is thus context-dependent.<sup>50</sup>

In conclusion, our findings offer insights into the contribution of miRNA unsilencing to the epigenetic therapy of lung cancer, and suggest that miRNAs of the chromosome 19 clusters may exert context-dependent anti-tumoral effects on lung cancer cells and may thus be considered as potential therapeutic agents in particular types of cancer.

## Materials and Methods

**Cell culture and chemicals.** Cell lines were maintained at 37 °C in a 5% CO<sub>2</sub> humidified incubator. A549, H460, HCT116, HeLa and HepG2 cells were grown in DMEM medium (Biological Industries, Kibbutz Beit-Haemek, Israel) supplemented with 10% heat-inactivated fetal bovine serum (GIBCO-BRL, Grand Island, NY, USA) and antibiotics (Biological Industries). H1299, H661, COR-L23 and SK-MEL-5 cells were grown in RPMI (Biological Industries) supplemented with 10% heat-inactivated fetal bovine serum and antibiotics. MRC5 cells were grown in

Minimal Essential Medium (Biological Industries) supplemented with 10% non-heat-inactivated fetal bovine serum, MEM-Eagle's nonessential amino acids, sodium pyruvate, L-glutamine and antibiotics. HBECs immortalized with hTERT+Cdk4<sup>51</sup> were grown in keratinocyte serum-free medium (Invitrogen, Grand Island, NY, USA) supplemented with 50  $\mu$ g/ml bovine Pituitary extract and 5 ng/ml hEGF (Invitrogen).<sup>52</sup>

5'aza-deoxycytidine (5'aza; MP Bio-Med, Santa Ana, CA, USA) was dissolved in acetic acid:H<sub>2</sub>O. Unless mentioned otherwise, cells were treated with 1  $\mu$ M 5'aza for 24 h. 0.1  $\mu$ M TSA (Sigma Aldrich, St. Louis, MO, USA) was then added for an additional 48 h, and medium was replaced daily. Cisplatin (cis) was applied to the cells for 48 h at a final concentration of 4  $\mu$ g/ml. Vorinostat (SAHA) was purchased from Selleck Chemicals (Houston, TX, USA).

**Transfections.** For siRNA or miR-mimics oligonucleotide transfections, Dharmafect 1 reagent (Dharmacon, Lafayette, CO, USA) was used according to the manufacturer's protocol. RelA siRNA was purchased from Dharmacon as Smartpool. Mature miR-mimic oligonucleotides and biotinylated mature miR-mimics were purchased from Dharmacon. For DNA transfections, JET-PEI reagent (PolyPlus, Illkirch, France) was used according to the manufacturer's protocol. A synthetic TEAD luciferase reporter (8XGTIIc-lux) was purchased from Addgene (Cambridge, MA, USA). pRL-TK (Renilla) was from Promega (Nacka, Sweden).

**Cell cycle analysis.** Cells were trypsinized, combined with floaters, washed once with ice-cold PBS, fixed in cold methanol for no less than 30 min, washed, rehydrated and resuspended in PBS containing 50  $\mu$ g/ml propidium iodide and 50  $\mu$ g/ml RNase A. Samples were analyzed in an LSRII (Becton Dickinson, Franklin Lakes, NJ, USA) flow cytometer.

**Western blot analysis.** Western blot analysis was performed as described.<sup>53</sup> For detection of pAkt and total Akt, cells were incubated for 20 h with medium supplemented with 0.5% serum, and then treated with 10 ng/ml insulin (Sigma Aldrich), harvested in sample buffer, boiled and sonicated for 5 min.

The following antibodies were used: GAPDH (Millipore, Billerica, MA, USA), RelA (Santa Cruz, Santa Cruz, CA, USA), PIK3CA (Santa Cruz), pRb (BD Pharmingen, San Jose, CA, USA),  $\beta$ -tubulin (Sigma Aldrich), Akt1 (Cell Signaling Eldan Ltd., Petach-Tiqva, Israel), pAkt ser473 (Cell Signaling Eldan Ltd.) and TEAD4 (Abcam, Cambridge, UK). Quantification of bands were performed using Image J software (NIH).

**RNA isolation and quantification.** Total RNA was isolated with a mirVana miRNA isolation kit (Invitrogen). For quantitative reverse transcriptase PCR (qRT-PCR), 1.5  $\mu$ g aliquots of RNA were reverse-transcribed using Moloney murine leukemia virus reverse transcriptase (Promega) and random hexamer primers (Amersham, Pittsburgh, PA, USA). qPCR was performed with SYBR Green Master Mix (Applied Biosystems, Foster City, CA, USA) in a StepOnePlus instrument (Applied Biosystems). The sequences of the qRT-PCR primers: GAPDH 5'GTCG GAGTCAACGGATTGG'3, 5'AAAAGCAGCCCTGGTGACC'3; IL-6 5'AGCCCTGA GAAAGGAGACATGTA'3, 5'TCTGCCAGTGCCTCTTTGCT'3; ITG $\alpha$ 11 5'GCAC CCCATTTCCAAACAAC'3, 5'ACCGCTCTCATCCATGGT'3; RelA 5'CTCCGGG GGCAGCAT'3, 5'TCCTGTGTAGCCATTGATCTTGAT'3; TEAD4 5'CAAGCAGGT GGTGGAGAAAG'3, 5'ATGTACTCACAGAGCGGGGA'3; CTGF 5'GCAGAGCCG CCTGTGCATGG'3, 5'GGTATGTCTTCATGCTGG'3; PIK3CA 5'AGGCTTGA TCTTCGAATGTTACCTT'3, 5'ATTTGCGACCACCTCAATAAGT'3; Bax 5'TGAGC AGATCATGAAGACAGGG'3, 5'GCTCGATCCTGGATGAAACC'3; CD95 5'TGAC ACTGGCAAACAATGCA'3, 5'GGTCTTTTACCAGCAAGCT'3.

For miR qPCR, reverse transcription and qPCR analysis were carried out with TaqMan MicroRNA assays (Applied Biosystems) according to the manufacturer's protocol. For pri-miR qPCR, RNA was first treated with 'TURBO DNase' (Applied Biosystems) and then subjected to reverse transcription. qPCR was performed using TaqMan Pri-MiRNA assays (Applied Biosystems) according to the manufacturer's protocol.

**miR microarray and mRNA expression array analysis.** miR profiling was performed with the following conditions: si-con, si-con+cis, si-con+5'aza+TSA, si-con+5'aza+TSA+cis, si-p53, si-p53+cis, si-p53+5'aza+TSA, si-p53+5'aza+TSA +cis, each in two biological replicates (total of 16 arrays) employing the Agilent (Santa Clara, CA, USA) platform. All arrays were normalized together using a Lowess multi-array algorithm. MiRs that were undetected in all samples (according to GeneView flags) were removed and all values lower than 10 (linear scale) were considered below detection and thresholded to 10. Duplicate samples were averaged to reduce noise, except for one condition (si-con+cis) for which one sample was excluded owing to a defective array.

mRNA expression analysis of si-control and si-p53 cells with or without 5'aza-TSA treatment was performed in triplicate, employing Affymetrix exon arrays (Santa Clara, CA, USA). mRNA expression data were analyzed as described.<sup>54</sup> Briefly, the Affymetrix Expression Console was used for summarization, and then all arrays were log<sub>2</sub>-transformed, normalized together, using a Lowess multi-array algorithm and thresholded at 4 (log<sub>2</sub> scale). Annotation and signal-based information was used to define exonic and intronic probe-sets. As there was a strong batch effect between the biological triplicates, we did not average the samples from each condition together, but instead found the differentially expressed genes in each biological replicate alone (absolute fold change > = 1.5) and intersected the lists of the three replicates.

mRNA expression levels of cells transfected with miR-512-5p and miR-373 mimic oligonucleotides or mimic-control oligonucleotides were measured in biological duplicates (for each mimic) by hybridization with Affymetrix Hu-Gene ST 1.0 arrays. Affymetrix Expression Console was used for summarization, and then all arrays were normalized together using a Lowess multi-array algorithm. The data were thresholded at 3 (log<sub>2</sub> scale).

**Sorting points into neighborhood.** This is an unsupervised method for sorting and visualization of multidimensional data.<sup>55</sup> The algorithm iteratively creates an optimal ordering of the objects being studied, such that the distances are small close to the diagonal of the pairwise distance matrix and increase as they move away from it. This ordering allows for finding groups of genes/miRs that display similar expression patterns over a range of samples.

**Exosome RNA isolation.** The medium of control and treated cells was replaced with serum-free medium for 24 h. The conditioned medium was collected and centrifuged at 3000 × g for 15 min. Exosomes were isolated from the supernatant with ExoQuick-TC kit (SBI, Mountain View, CA, USA) according to the manufacturer's protocol. RNA was isolated and quantified as described above.

**Senescence-associated β-galactosidase assay.** Cells were washed once with PBS, fixed with 0.5% glutaraldehyde (in PBS, pH 7.4) for 15 min at room temperature, and washed in PBS (pH 6.0) supplemented with 1 mM MgCl<sub>2</sub>. Cells were incubated with X-gal solution (1 mg/ml X-gal (Inalco, San Luis Obispo, CA, USA), 0.2 M K<sub>3</sub>Fe(CN)<sub>6</sub>, 0.2 M K<sub>4</sub>Fe(CN)<sub>6</sub>·3H<sub>2</sub>O) for 4 h at 37 °C, and then washed with PBS and incubated with 3.7% formalin (in PBS) for 30 min at room temperature. Images were taken using Olympus microscope (Tokyo, Japan). Images were analyzed using CellP software (Diagnostic Instruments, Tokyo, Japan).

**Migration assays.** Experiments were carried out using an xCELLigence Real-Time Cell Analysis DP instrument (Roche Diagnostics GmbH, Mannheim, Germany), placed in a humidified incubator at 37 °C with 5% CO<sub>2</sub>. Initially, 160 μl of medium and 30 μl of serum-free medium was added to the lower and upper chambers of modified 16-well plates (CIM-16, Roche Diagnostics GmbH), respectively, and incubated in the Real Time Cell Analyzer device for 1 h to obtain equilibrium according to the manufacturer's guidelines. Then, background signal was determined with cell-free medium. To initiate an experiment, cells were trypsinized, resuspended in serum-free medium and seeded in the upper chambers (8 × 10<sup>5</sup> cells/chamber). Plates were incubated for 30 min in a laminar flow hood to allow the cells to settle onto the membrane, and then locked in the Real Time Cell Analyzer device. The impedance of each well was automatically measured every 15 min for a total period of 25 h and expressed as Cell Index Value.

**BrdU analysis.** Cells were pre-labeled with 10 μM BrdU (Sigma Aldrich). After 60 min, cells were trypsinized, collected and fixed with 70% ethanol/HBSS overnight at -20 °C. Fixed cells were denatured in 2N HCl, 0.5% Triton in PBS for 30 min at room temperature and then neutralized with 0.1 M Na<sub>2</sub>B<sub>4</sub>O<sub>7</sub> (pH 8.5), incubated with anti-BrdU antibodies (Becton Dickinson) for 1 h, and resuspended in 50 μg/ml propidium iodide and 50 μg/ml RNase A. BrdU incorporation was analyzed in an LSRII (Becton Dickinson) flow cytometer.

**Colony-formation assay.** Twenty-four hours following transfection, cells were trypsinized and re-seeded in 10 cm plates at a density of 3000 cells per plate. For crystal violet staining, plates were washed once with PBS and once with cold methanol and then incubated in crystal violet (0.3% in methanol) for 5 min at -20 °C. Plates were subsequently washed with double distilled water, air-dried and scanned using a Canon scanner (Tokyo, Japan).

**Bisulfite pyrosequencing.** One microgram of genomic DNA was treated with bisulfite, using an EpiTect Bisulfite kit (Qiagen, Valencia, CA, USA) according to

the manufacturer's instructions. Primers were designed using the PyroMark Assay Design 2.0 software (Biotage, Uppsala, Sweden). PCR primers for amplification of bisulfite-treated DNA were: miR-373 promoter 5'ATGGAGGAGTTAATTTG TTTTGGGGTAT'3, 5'AACCTAAATAACAAAACCAATCCTATCT'3; miR-512 promoter region A: 5'ATGTTGGTTTAGGTGGTAAAGAA'3, 5'CCCCAATACCAAACTCA CTT'3; miR-512 promoter region B: 5'GGGGTATAGTGGGGATATATATGA'3, 5'AAACCAACATCTTAATCCCTTTTA'3.

PCR amplicons were amplified from bisulfite-treated DNA using Maxima HotStartTaq (Fermentas, Pittsburgh, PA, USA). DNA was extracted with NucleoSpin Gel and PCR Clean-up (MACHEREY-NAGEL, Duren, Germany). Pyrosequencing reactions were performed on a PyroMark Q24 pyrosequencer (Qiagen) using 2 pmol of the biotinylated purified PCR products according to the manufacturer's instructions. Sequencing primers: miR-373 5'GTTTTTGGGGTATTTTGG'3; miR-512A 5'GTGTAAAGAAAGGTG'3; miR-512B 5'GGGGATATATATTTGATTG'3.

**Biotin miR pulldown.** The biotinylated-miR pulldown assay was adapted from Lal et al.<sup>33</sup> Briefly, HepG2 cells (1 × 10<sup>6</sup>) were transfected with 100 nM biotin-control-mimic or biotin-373-mimic oligonucleotides. Forty-eight hours later, cells were trypsinized and resuspended in 1 ml lysis buffer (20 mM Tris (pH 7.5), 100 mM KCl (Ambion, Grand Island, NY, USA), 5 mM MgCl<sub>2</sub> (Ambion), 0.3% NP-40) supplemented with 100 U of RNasin (Promega) and protease inhibitor cocktail, and incubated on ice for 20 min. The cytoplasmic lysate was isolated by centrifugation at 10 000 × g for 15 min. Streptavidin-coated magnetic beads (Invitrogen) were blocked for 1 h at 4 °C in lysis buffer containing 1 mg/ml yeast tRNA and 1 mg/ml BSA (Ambion) and washed twice with lysis buffer. Cytoplasmic lysate was added to the beads and incubated for 4 h at 4 °C. Beads were washed five times with lysis buffer. RNA bound to the beads as well as 10% of the extract (input RNA) was isolated using Trizol (Invitrogen) and chloroform (Fisher Scientific, Waltham, MA, USA). Pulled-down mRNA was quantified by qRT-PCR. Values were normalized to GAPDH in the same sample and then to input (cellular RNA without incubation with beads).

**Luciferase assays.** Cells were plated at a density of 64 × 10<sup>3</sup> in 12-well plates, and transfected 24 h later in triplicate with 20 nM miR-mimics. After an additional 24 h, cells were transfected with 300 ng/well DNA of psiCHECK2 reporter plasmid containing the PK3CA-3'UTR or the TEAD4-3'UTR downstream to the Renilla luciferase coding region, or with a TEAD-luciferase reporter (8XGTIC-lux) (300 ng/well) together with pRL-TK control plasmid (20 ng/well). Twenty-four hours later, cells were harvested with the Dual luciferase reporter assay system (Promega) according to the manufacturer's instructions. Luciferase and Renilla bioluminescence were measured in an Infinite M200 microplate reader (Tecan, Männedorf, Switzerland).

**Mice.** Mouse experiments were approved by the Weizmann Institutional Animal Care and Use Committee (IACUC). Procedures were performed under anesthesia (100 mg/Kg Ketamine intraperitoneally; Fort Dodge Animal Health). H460 cells stably expressing luciferase were treated with 5'aza-TSA or with acetic acid, as described above. At the end of the treatment, 3 × 10<sup>6</sup> cells were injected subcutaneously in 50 μl PBS into the hind limb of male CD1 nude mice (Harlan Laboratories, Indianapolis, IN, USA). Procedures involving animals were approved by the Animal Ethics Committee of the Weizmann Institute (Institutional Animal Care and Use Committee) and conformed to the guidelines of the Israel Council for Experiments in Animals.

**In vivo imaging.** Tumor growth was monitored using the IVIS spectrum bioluminescence imaging system (Caliper Life Sciences, Waltham, MA, USA). Mice were imaged following intraperitoneal injection of 1.5 mg of D-luciferin (Caliper Life Sciences). Measurements were performed when the signal reached maximal plateau. A region of interest was defined for each tumor, and average radiance (p/s/cm<sup>2</sup>/sr) values were extracted for quantification.

**Statistical analysis.** Statistical significance was determined using Student's-t test. P < 0.05 (\*), P < 0.005 (\*\*), and P < 0.0005 (\*\*\*) were considered as significant (asterisks refer to all figures).

#### Conflict of Interest

The authors declare no conflict of interest.

**Acknowledgements.** We thank V. Gorgoulis for the kind gift of immortalized HBECS. This work was supported in part by the Dr Miriam and Sheldon Adelson Medical Research Foundation, EC FP7 grant 201102 (ONCOMIRS), a Center of



Excellence grant from the Flight Attendant Medical Research Institute (FAMRI), the Robert Bosch Foundation (project 11.5.8000.0094.0), the Leir Charitable Foundation, The M.D. Moross Institute for Cancer Research and the McGill-Weizmann Collaboration Program. ED is incumbent of the Henry J. Leir Professorial Chair. MO is incumbent of the Andre Lwoff chair in Molecular Biology.

- Katayama R, Shaw AT, Khan TM, Mino-Kenudson M, Solomon BJ, Halmos B *et al*. Mechanisms of acquired crizotinib resistance in ALK-rearranged lung Cancers. *Sci Transl Med* 2012; **4**: 120ra17.
- Liu HP, Isaac Wu HD, Chang JW, Wu YC, Yang HY, Chen YT *et al*. Prognostic implications of epidermal growth factor receptor and KRAS gene mutations and epidermal growth factor receptor gene copy numbers in patients with surgically resectable non-small cell lung cancer in Taiwan. *J Thorac Oncol* 2010; **5**: 1175–1184.
- Baylin SB, Jones PA. A decade of exploring the cancer epigenome—biological and translational implications. *Nat Rev Cancer* 2011; **11**: 726–734.
- Bergman Y, Cedar H. DNA methylation dynamics in health and disease. *Nat Struct Mol Biol* 2013; **20**: 274–281.
- Aran D, Hellman A. DNA methylation of transcriptional enhancers and cancer predisposition. *Cell* 2013; **154**: 11–13.
- Barneda-Zahonero B, Parra M. Histone deacetylases and cancer. *Mol Oncol* 2012; **6**: 579–589.
- Kaminsky VO, Surova OV, Vaculova A, Zhivotovsky B. Combined inhibition of DNA methyltransferase and histone deacetylase restores caspase-8 expression and sensitizes SCLC cells to TRAIL. *Carcinogenesis* 2011; **32**: 1450–1458.
- Iorio MV, Croce CM. Causes and consequences of microRNA dysregulation. *Cancer J* 2012; **18**: 215–222.
- Hatley ME, Patrick DM, Garcia MR, Richardson JA, Bassel-Duby R, van Rooij E *et al*. Modulation of K-Ras-dependent lung tumorigenesis by MicroRNA-21. *Cancer Cell* 2010; **18**: 282–293.
- Lu J, Getz G, Miska EA, Alvarez-Saavedra E, Lamb J, Peck D *et al*. MicroRNA expression profiles classify human cancers. *Nature* 2005; **435**: 834–838.
- Biagioni F, Bossel Ben-Moshe N, Fontemaggi G, Canu V, Mori F, Antoniani B *et al*. miR-10b\*, a master inhibitor of the cell cycle, is down-regulated in human breast tumours. *EMBO Mol Med* 2012; **4**: 1214–1229.
- Davalos V, Moutinho C, Villanueva A, Boque R, Silva P, Carneiro F *et al*. Dynamic epigenetic regulation of the microRNA-200 family mediates epithelial and mesenchymal transitions in human tumorigenesis. *Oncogene* 2012; **31**: 2062–2074.
- Rauhala HE, Jalava SE, Isotalo J, Bracken H, Lehmusvaara S, Tammela TL *et al*. miR-193b is an epigenetically regulated putative tumor suppressor in prostate cancer. *Int J Cancer* 2010; **127**: 1363–1372.
- Laurent LC, Chen J, Ulitsky I, Mueller FJ, Lu C, Shamir R *et al*. Comprehensive microRNA profiling reveals a unique human embryonic stem cell signature dominated by a single seed sequence. *Stem Cells* 2008; **26**: 1506–1516.
- Hanahan D, Weinberg RA. Hallmarks of cancer: the next generation. *Cell* 2011; **144**: 646–674.
- Campisi J, Andersen JK, Kapahi P, Melov S. Cellular senescence: a link between cancer and age-related degenerative disease? *Semin Cancer Biol* 2011; **21**: 354–359.
- Campisi J, d'Adda di Fagagna F. Cellular senescence: when bad things happen to good cells. *Nat Rev Mol Cell Biol* 2007; **8**: 729–740.
- Reguart N, Rosell R, Cardenal F, Cardona AF, Isla D, Palmero R *et al*. Phase III trial of vorinostat (SAHA) and erlotinib for non-small cell lung cancer (NSCLC) patients with epidermal growth factor receptor (EGFR) mutations after erlotinib progression. *Lung Cancer* 2014; **84**: 161–167.
- Tsai KW, Kao HW, Chen HC, Chen SJ, Lin WC. Epigenetic control of the expression of a primate-specific microRNA cluster in human cancer cells. *Epigenetics* 2009; **4**: 587–592.
- Zhou AD, Diao LT, Xu H, Xiao ZD, Li JH, Zhou H *et al*. beta-Catenin/LEF1 transactivates the microRNA-371-373 cluster that modulates the Wnt/beta-catenin-signaling pathway. *Oncogene* 2012; **31**: 2968–2978.
- Saito Y, Suzuki H, Tsugawa H, Nakagawa I, Matsuzaki J, Kanai Y *et al*. Chromatin remodeling at Alu repeats by epigenetic treatment activates silenced microRNA-512-5p with downregulation of Mcl-1 in human gastric cancer cells. *Oncogene* 2009; **28**: 2738–2744.
- Tanaka T, Arai M, Wu S, Kanda T, Miyauchi H, Imazeki F *et al*. Epigenetic silencing of microRNA-373 plays an important role in regulating cell proliferation in colon cancer. *Oncol Rep* 2011; **26**: 1329–1335.
- Pigati L, Yaddanapudi SC, Iyengar R, Kim DJ, Hearn SA, Danforth D *et al*. Selective release of microRNA species from normal and malignant mammary epithelial cells. *PLoS One* 2010; **5**: e13515.
- Rabinowitz G, Gercel-Taylor C, Day JM, Taylor DD, Kloecker GH. Exosomal microRNA: a diagnostic marker for lung cancer. *Clin Lung Cancer* 2009; **10**: 42–46.
- Zhu CQ, Popova SN, Brown ER, Barsyte-Lovejoy D, Navab R, Shih W *et al*. Integrin alpha 11 regulates IGF2 expression in fibroblasts to enhance tumorigenicity of human non-small-cell lung cancer cells. *Proc Natl Acad Sci U S A* 2007; **104**: 11754–11759.
- Huang Q, Gumireddy K, Schrier M, le Sage C, Nagel R, Nair S *et al*. The microRNAs miR-373 and miR-520c promote tumour invasion and metastasis. *Nat Cell Biol* 2008; **10**: 202–210.
- Keklikoglou I, Koerner C, Schmidt C, Zhang JD, Heckmann D, Shavinskaya A *et al*. MicroRNA-520/373 family functions as a tumor suppressor in estrogen receptor negative breast cancer by targeting NF-kappaB and TGF-beta signaling pathways. *Oncogene* 2012; **31**: 4150–4163.
- Voorhoeve PM, le Sage C, Schrier M, Gillis AJ, Stoop H, Nagel R *et al*. A genetic screen implicates miRNA-372 and miRNA-373 as oncogenes in testicular germ cell tumors. *Cell* 2006; **124**: 1169–1181.
- Huang da W, Sherman BT, Lempicki RA. Bioinformatics enrichment tools: paths toward the comprehensive functional analysis of large gene lists. *Nucleic Acids Res* 2009; **37**: 1–13.
- Huang da W, Sherman BT, Lempicki RA. Systematic and integrative analysis of large gene lists using DAVID bioinformatics resources. *Nat Protoc* 2009; **4**: 44–57.
- Perkins ND. The diverse and complex roles of NF-kappaB subunits in cancer. *Nat Rev Cancer* 2012; **12**: 121–132.
- Tang X, Liu D, Shishodia S, Ozburn N, Behrens C, Lee JJ *et al*. Nuclear factor-kappaB (NF-kappaB) is frequently expressed in lung cancer and preneoplastic lesions. *Cancer* 2006; **107**: 2637–2646.
- Lal A, Thomas MP, Altschuler G, Navarro F, O'Day E, Li XL *et al*. Capture of microRNA-bound mRNAs identifies the tumor suppressor miR-34a as a regulator of growth factor signaling. *PLoS Genet* 2011; **7**: e1002363.
- Katso R, Okkenhaug K, Ahmadi K, White S, Timms J, Waterfield MD. Cellular function of phosphoinositide 3-kinases: implications for development, homeostasis, and cancer. *Annu Rev Cell Dev Biol* 2001; **17**: 615–675.
- McCubrey JA, Steelman LS, Chappell WH, Abrams SL, Montalto G, Cervello M *et al*. Mutations and deregulation of Ras/Raf/MEK/ERK and PI3K/PDEN/Akt/mTOR cascades which alter therapy response. *Oncotarget* 2012; **3**: 954–987.
- Zhao B, Ye X, Yu J, Li L, Li W, Li S *et al*. TEAD mediates YAP-dependent gene induction and growth control. *Genes Dev* 2008; **22**: 1962–1971.
- Zhao B, Li L, Lei Q, Guan KL. The Hippo-YAP pathway in organ size control and tumorigenesis: an updated version. *Genes Dev* 2010; **24**: 862–874.
- Lu F, Zhang HT. DNA methylation and non-small cell lung cancer. *Anat Rec* 2011; **294**: 1787–1795.
- Crea F, Nobili S, Paolicchi E, Perrone G, Napoli C, Landini I *et al*. Epigenetics and chemoresistance in colorectal cancer: an opportunity for treatment tailoring and novel therapeutic strategies. *Drug Resist Updat* 2011; **14**: 280–296.
- Juergens RA, Wrangle J, Vendetti FP, Murphy SC, Zhao M, Coleman B *et al*. Combination epigenetic therapy has efficacy in patients with refractory advanced non-small cell lung cancer. *Cancer Discov* 2011; **1**: 598–607.
- Ramachandran K, Gordian E, Singal R. 5-azacytidine reverses drug resistance in bladder cancer cells. *Anticancer Res* 2011; **31**: 3757–3766.
- Steele N, Finn P, Brown R, Plumb JA. Combined inhibition of DNA methylation and histone acetylation enhances gene re-expression and drug sensitivity in vivo. *Br J Cancer* 2009; **100**: 758–763.
- Lu Y, Govindan R, Wang L, Liu PY, Goodgame B, Wen W *et al*. MicroRNA profiling and prediction of recurrence/relapse-free survival in stage I lung cancer. *Carcinogenesis* 2012; **33**: 1046–1054.
- Seol HS, Akiyama Y, Shimada S, Lee HJ, Kim TI, Chun SM *et al*. Epigenetic silencing of microRNA-373 to epithelial-mesenchymal transition in non-small cell lung cancer through IRAK2 and LAMP1 axes. *Cancer Lett* 2014; **353**: 232–241.
- Liang G, Gonzales FA, Jones PA, Orntoft TF, Thykjaer T. Analysis of gene induction in human fibroblasts and bladder cancer cells exposed to the methylation inhibitor 5-aza-2'-deoxycytidine. *Cancer Res* 2002; **62**: 961–966.
- Paskova L, Smesny Trtkova K, Fialova B, Benedikova A, Langova K, Kolar Z. xDifferent effect of sodium butyrate on cancer and normal prostate cells. *Toxicol In Vitro* 2013; **27**: 1489–1495.
- Glazer CA, Smith IM, Ochs MF, Begum S, Westra W, Chang SS *et al*. Integrative discovery of epigenetically derepressed cancer testis antigens in NSCLC. *PLoS One* 2009; **4**: e8189.
- Rippe V, Dittberner L, Lorenz VN, Drieschner N, Nimzyk R, Sendt W *et al*. The two stem cell microRNA gene clusters C19MC and miR-371-3 are activated by specific chromosomal rearrangements in a subgroup of thyroid adenomas. *PLoS One* 2010; **5**: e9485.
- Nakata K, Ohuchida K, Mizumoto K, Aishima S, Oda Y, Nagai E *et al*. Micro RNA-373 is down-regulated in pancreatic cancer and inhibits cancer cell invasion. *Ann Surg Oncol* 2014; **21**(Suppl 4): 564–574.
- Kasinski AL, Slack FJ. Epigenetics and genetics. MicroRNAs en route to the clinic: progress in validating and targeting microRNAs for cancer therapy. *Nat Rev Cancer* 2011; **11**: 849–864.
- Ramirez RD, Sheridan S, Girard L, Sato M, Kim Y, Pollack J *et al*. Immortalization of human bronchial epithelial cells in the absence of viral oncoproteins. *Cancer Res* 2004; **64**: 9027–9034.
- Velimezi G, Lontos M, Vougas K, Roumeliotis T, Bartkova J, Sideridou M *et al*. Functional interplay between the DNA-damage-response kinase ATM and ARF tumour suppressor protein in human cancer. *Nat Cell Biol* 2013; **15**: 967–977.
- Aylon Y, Michael D, Shmueli A, Yabuta N, Nojima H, Oren M. A positive feedback loop between the p53 and Lats2 tumor suppressors prevents tetraploidization. *Genes Dev* 2006; **20**: 2687–2700.
- Zeisel A, Kostler WJ, Molotski N, Tsai JM, Krauthgamer R, Jacob-Hirsch J *et al*. Coupled pre-mRNA and mRNA dynamics unveil operational strategies underlying transcriptional responses to stimuli. *Mol Syst Biol* 2011; **7**: 529.
- Tsafir D, Tsafir I, Ein-Dor L, Zuk O, Notterman DA, Domany E. Sorting points into neighborhoods (SPIN): data analysis and visualization by ordering distance matrices. *Bioinformatics* 2005; **21**: 2301–2308.

Supplementary Information accompanies this paper on Cell Death and Differentiation website (<http://www.nature.com/cdd>)